Applied Physics B (2022) 128:68
https://doi.org/10.1007/s00340-022-07780-4

Applied Physics B
Lasers and Optics

Laser-induced fluorescence for studying the influence of potassium and sodium salts on PAH formation in sooting premixed flames

Manu Mannazhi[1] · Saga Bergqvist[1] · Per-Erik Bengtsson[1]

Received: 11 November 2021 / Accepted: 7 February 2022 / Published online: 10 March 2022

Abstract
Previous studies have shown that alkali salts influence combustion processes and soot formation, although the effects seem to vary across systems. Moreover, fundamental studies on the effect of potassium and sodium salts on formation of polycyclic aromatic hydrocarbons (PAH), which are precursors in soot formation, are scarce. Here, we report a study in which the effects on PAH formation due to the addition of alkali metal salts (KCl, KOH, K_2CO_3, NaCl and NaOH) to premixed ethylene–air flames were investigated. Different size classes of PAHs were probed using both spectral and 2D measurements of laser-induced fluorescence (PAH-LIF) using the excitation wavelengths 266 nm and 532 nm, while detecting the fluorescence emission at selected wavelength ranges. Elastic light scattering (ELS) measurements were also used to complement the fluorescence data. It was found that potassium and sodium salts do not significantly influence the formation of small PAHs (2–3 rings), while decreasing the concentration of larger PAHs at higher heights above burner (HAB). Another important result was that the anion in the salt (Cl^-, OH^-, CO_3^{2-}) negligibly influences the PAH and soot formation processes after dissociation of the salts.

Abbreviations

ELS	Elastic light scattering
HAB	Height above burner
LIF	Laser-induced fluorescence
LIF266-BP320	Laser-induced fluorescence using excitation at 266 nm and detection at 320 nm
LIF532	Laser-induced fluorescence using excitation at 532 nm
PAH	Polycyclic aromatic hydrocarbon
K_2CO_3	Potassium carbonate
KCl	Potassium chloride
KOH	Potassium hydroxide
NaCl	Sodium chloride
NaOH	Sodium hydroxide

1 Introduction

The scientific community has been in the quest to decipher soot formation for several decades [1–3]. In recent years, soot formation related to biomass combustion and gasification processes have received increased attention [4–6] due to the renewable nature of biomass which potentially makes them one of the main contributors in replacing fossil fuel based (non-renewable) combustion systems. Biomass combustion/gasification systems are complex systems involving solid fuels (of various sizes), and commonly used biomass sources such as pinewood, beechwood, wheat straw, etc. contain substantial amounts of trace elements including various metals with large variation between feedstock [7, 8]. For example, various biomass feedstocks were found to have potassium concentrations in the range 300–1700 ppm, sodium concentrations in the range 20–120 ppm, and chlorine concentrations up to 300 ppm [9].

There have been several studies on the influence of potassium and sodium on soot formation in applied systems, such as biomass and coal combustion systems [7, 10–18]. For example, addition of potassium has been found to reduce soot concentration [7], diminish particulate matter emissions [10] and improve catalytic activity in soot oxidation process [10–13]. Likewise, sodium addition also showed catalytic activity for soot oxidation [14, 15], and an increase in soot yield [15]. However, the effects of addition of potassium or sodium are found to vary across systems. For example, potassium chloride (KCl) impregnation of birch wood in a wood stove increased the emission of larger particles (size ~ 200–500 nm) while reducing the emission of

✉ Manu Mannazhi
manu.mannazhi@gmail.com

[1] Division of Combustion Physics, Department of Physics, Lund University, Box 118, 221 00 Lund, Sweden

ultrafine particles [16]. In another study, Na addition promoted soot formation at low temperatures while inhibiting the same at higher temperatures (> 1373 K) [17]. Hence, there is a motivation for more fundamental understanding of the underlying soot formation processes, and to get further insight simplified laboratory scale systems have often been used in combination with advanced optical/laser diagnostic methods.

Several fundamental studies have been performed in well-characterized flames on laboratory burners to investigate the influence of potassium and sodium on soot formation [19–28]. Addition of KCl to partially premixed ethylene–air flames was found to reduce soot volume fraction while showing negligible effects on primary and sub-primary particle sizes [19]. However, an earlier study showed that addition of sodium and potassium salts into premixed ethylene–air flames resulted in smaller soot particles [20]. In another study, addition of KCl and potassium hydroxide (KOH) promoted the formation of acetylene and benzene, while KOH also showed an increase in the soot volume concentration and particle size [21]. Likewise, addition of sodium chloride to flames have shown varying trends for soot concentration (increase [22] and decrease [23]) and soot oxidation (promotion [24] and inhibition [25]). Hence, despite these fundamental investigations there are still ambiguities in the effect of trace elements on soot formation.

In our previous work, fundamental studies were performed by aspirating chlorides of various metals (including KCl and NaCl) into sooting premixed ethylene–air flames ($\Phi = 2.6$) [26, 27]. The techniques laser-induced incandescence (LII), elastic light scattering (ELS), and laser extinction were used in-situ in the flames along with transmission electron microscopy (TEM) on sampled soot to study the effects of these salt additives on soot formation. Addition of KCl resulted in a significant decrease in soot volume fraction (f_v), while NaCl addition led to a small decrease of f_v at high concentrations. It was also found that while KCl addition reduced the soot primary particle sizes, NaCl had a negligible effect. However, the work in [19, 20] does not uncover the effect of chloride ions (Cl^-) in soot formation (as all the salts were chlorides). In some earlier studies, it has been shown that chlorine addition tends to increase soot formation [29, 30]. In addition, some of the effects of salt addition seem to change with anions (for example, KOH increased particle size [21]), while some others remain the same (for example, catalytic behaviour [18]). Thus, to gain a deeper understanding of the effects of these added salts on soot formation, it is of great value to perform experiments, where the anion in the salt is varied. In addition, it is of great interest to investigate how different salts (with various alkali metals and various anions) influence in the formation of polycyclic aromatic hydrocarbons (PAHs), which are considered as precursors of soot [31].

Polycyclic aromatic hydrocarbons (PAHs) can be studied non-intrusively using laser-induced fluorescence (LIF) [31, 32], here denoted as PAH-LIF. PAH-LIF has low specificity as the fluorescence emission from different PAHs are spectrally overlapping [33], and dependent on excitation wavelength [34] and temperature [33, 35]. PAHs fluoresce in a wide range of excitation wavelengths from 250 nm [34] to 680 nm [32]. Although 266 nm is likely to excite most of the PAHs irrespective of their sizes [32], larger PAHs are generally excited by longer wavelengths [36]. In addition, the fluorescence response of PAHs shift towards larger wavelengths with increase in their molecular sizes [36–39]. Laser excitation using 266 nm is shown to produce bimodal signal distribution with a UV peak at ~ 320 nm and a broader peak in the visible region between 400 and 600 nm [32, 39–43]. PAH-LIF emission in the UV and visible regions are considered to be, respectively, from small (2–3 rings) and larger PAH species [39, 40, 42, 44, 45] (and PAH dimers [46]). Thus, PAH-LIF measurements performed using more than one excitation wavelength while detecting the signal at different wavelength ranges can provide information about the various size classes of PAHs.

The present study is a continuation of previous work [28], where PAH-LIF measurements on premixed ethylene–air flames added with KCl showed that KCl negligibly influences the formation of smaller PAHs while decreasing the formation of larger PAHs. In the present study, the influence of various potassium and sodium salts on PAH formation was investigated. Various concentrations of aqueous solutions of five salts (KCl, KOH, K_2CO_3, NaCl and NaOH) were aspirated into premixed ethylene–air flames. PAH-LIF measurements were performed using the excitation wavelengths 266 nm and 532 nm while detecting the fluorescence emission at selected wavelength ranges to characterize different size classes of PAHs. In addition to the investigation of the effects of K and Na on PAH formation, the influence of the anion in the salt (Cl^-, OH^-, CO_3^{2-}) on PAH formation in sooting flames was also explored in this study.

2 Experimental setup

Investigations reported in this work were performed in premixed ethylene–air flames ($\Phi = 2.6$) stabilized on a Perkin–Elmer burner. This equivalence ratio was chosen to replicate the reference flame conditions in the study reported in [26, 27]. In this water-cooled burner, the premixed ethylene and air pass through a region of a metallic grid 23 mm in diameter with flow rates of 0.27 l/min and 1.5 l/min (at 273 K and 1 atm), respectively. Meanwhile, co-flow of air introduced to stabilize the flame passes through a concentric outer region with a diameter of 45 mm with a flow rate of 9 l/min (at 273 K and 1 atm). Moreover, a stainless-steel

flame stabilizer was placed 21 mm above the burner surface. A reference case (deionized water) and 1 M, 0.1 M and 0.01 M solutions of KCl, KOH, NaCl and NaOH prepared in deionized water were aspirated to the fuel–air mixture. For K_2CO_3, 0.5 M, 0.05 M and 0.005 M solutions were prepared to have the same concentration of the metal ions in the solution compared to the other salt solutions. However, these concentrations will, respectively, be denoted as 1 M, 0.1 M and 0.01 M in this paper for convenience. The flow rate of the solutions were ~ 3 ml/hour leading to a potassium or sodium concentration of ~ 600 ppm in the flame for the 1 M case. Flame luminosity images of the reference and the 1 M cases of KCl and NaCl captured using a digital camera are shown in Fig. 1a.

A schematic representation of the experimental setup is given in Fig. 1b. Some important aspects of the setup are discussed here, while a more detailed description on the optical setup is given in [28]. PAH-LIF measurements were performed using Nd:YAG lasers (Quantel Brilliant-b, repetition rate 10 Hz) operated at the wavelengths 532 nm and 266 nm. The laser beams were spatially overlapped using dichroic mirrors and transformed into thin laser sheets at the centre of the burner using cylindrical ($f = -40$ mm) and spherical ($f = +500$ mm) lenses. The laser sheets illuminated a region approximately between 1 and 18 mm height above burner (HAB). To increase the signal intensity without causing soot incandescence, the 266 nm laser sheet was slightly defocused to increase the probe volume in the horizontal direction. Fluences as low as ~ 0.004 J/cm^2 and 0.02 J/cm^2 were used for the 266 nm and 532 nm laser sheets to avoid incandescence contribution from soot.

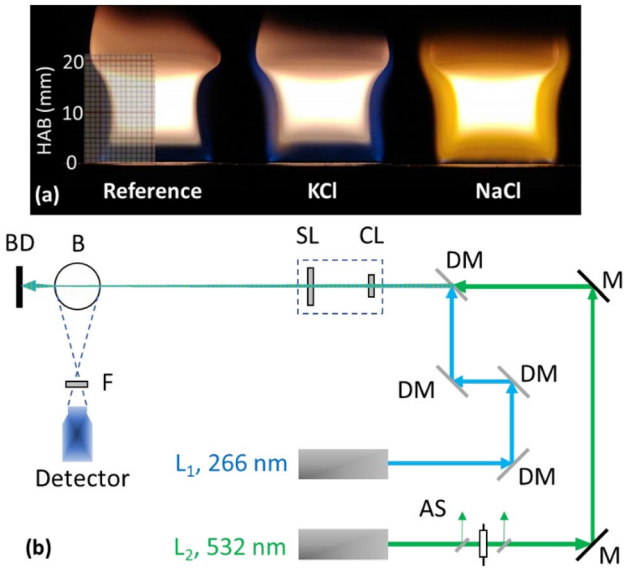

Fig. 1 **a** Flame luminosity images of the reference and 1 M cases of KCl and NaCl. **b** Schematic representation of the experimental setup. L, Nd:YAG laser; AS, attenuation system; M, mirror; DM, dichroic mirror; CL, cylindrical lens; SL, spherical lens; B, burner; F, optical filter; BD, beam dump; detector, ICCD camera or ICCD with spectrometer

Two-dimensional PAH-LIF signals were acquired using a PIMAX 4 ICCD camera equipped with a UV objective lens (B.Halle, $f = 100$ mm, f#2.0). 2D PAH-LIF signals obtained using the 266 nm laser excitation (denoted as *LIF266* from now on) were acquired at the wavelength 320 nm. This LIF signal corresponding to small PAHs (2–3 rings) [40, 42, 44, 45] was obtained using a band-pass filter with central wavelength at 320 nm having a bandwidth of 40 nm (denoted as *BP320*). For the PAH-LIF measurements using 532 nm excitation (denoted as *LIF532*), a notch filter at 532 nm (N532, OD ≥ 6.0 @ 532 nm, FWHM = 17 nm) was used to block the strong scattering signal from soot. Spatial non-uniformities of the laser intensities for both the LIF532 and LIF266 cases were corrected for using the LIF intensity profile from a Rhodamine–ethanol solution in a cuvette.

Spectral PAH-LIF data was acquired using an Acton SP-150 spectrometer in combination with the same ICCD camera and objective lens used in the imaging measurements. Laser wavelength of 266 nm was used for exciting the PAHs, and for acquiring the fluorescence spectra no optical filters were placed in front of the detector.

Elastic light scattering (ELS) measurements employed the same setup as the 2D LIF532 measurements barring a few exceptions in the signal acquisition part. Instead of the N532 filter, a band-pass filter at 532 nm (FWHM = 3 nm) was used, which blocked majority of the PAH-LIF signals. Furthermore, a linear polarizer was used to detect only the vertically scattered light to even further suppress potential light interferences.

For the PAH-LIF and ELS measurements, a prompt detection gate of 30 ns was used. In addition, semi-simultaneously acquired background luminosity images were subtracted from the averaged signal images of 300–500 single shots.

3 Results and discussion

The main results are presented as height profiles of the LIF signal intensity in Figs. 2 and 3. At lower heights there is a shift in the onset in PAH formation that we relate to the release of the ions in the salts due to dissociation, and this part of the profiles will be discussed separately in Sect. 3.4. Hence initially signal profiles vs height above 5 mm will be discussed in Fig. 2 and above 8 mm in Fig. 3.

The LIF signal intensity is detected in two different spectral regions corresponding to different size classes of PAHs, and the signal intensity in each region is related to the PAH concentration. For the data presented in Figs. 2 and 3, PAH-LIF signal intensity profiles along the height direction were obtained by averaging the 2D PAH-LIF signal intensity

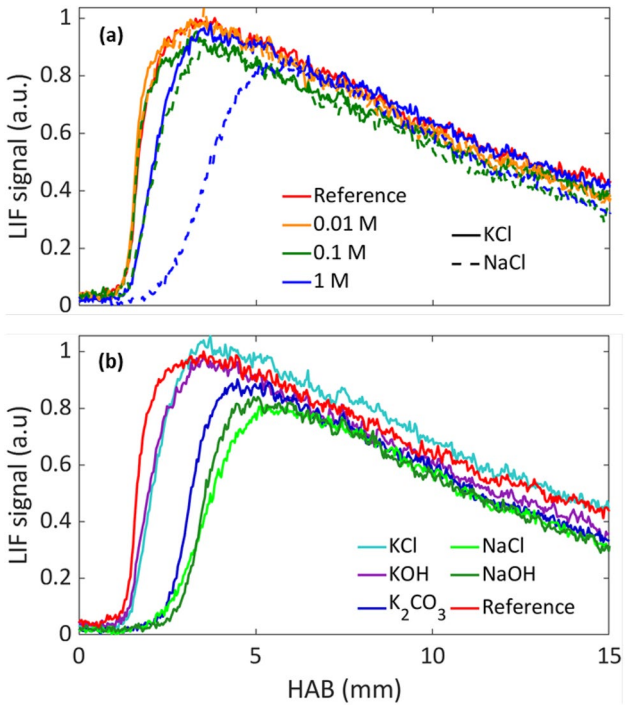

Fig. 2 Laser-induced fluorescence height profiles obtained after laser excitation at 266 nm and detection at 320 nm for **a** various concentration cases of KCl (solid lines) and NaCl (dotted lines) addition along with the reference case and **b** 1 M cases of all the salts along with the reference case

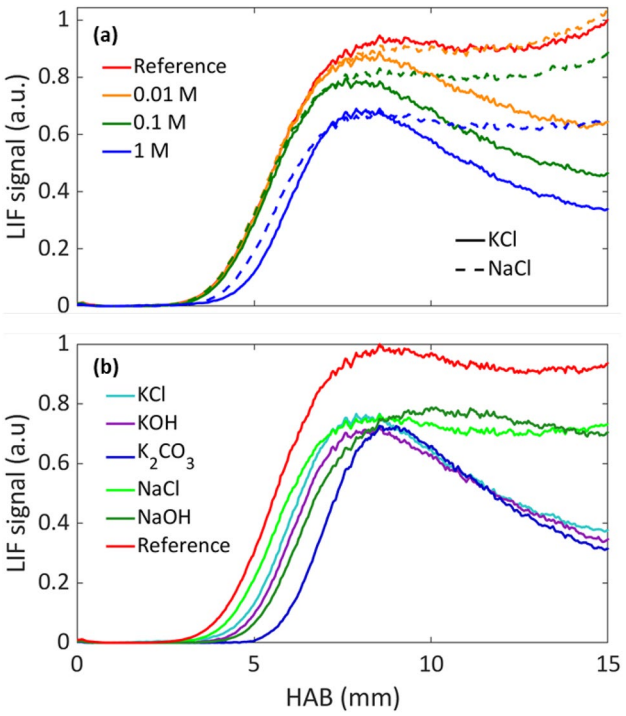

Fig. 3 Laser-induced fluorescence height profiles obtained after laser excitation at 532 nm for **a** various concentration cases of KCl (solid lines) and NaCl (dotted lines) addition along with the reference case and **b** 1 M cases of all the salts along with the reference case

images in the horizontal region over a distance of ~ 0.5 mm at the centre of the flame. The 2D images being symmetric also shows that there was negligible absorption of the laser energy across the diameter of the flame.

3.1 Excitation at 266 nm—detection at 320 nm

The LIF case corresponding to excitation at 266 nm and detection in the wavelength range 300 nm–340 nm is here denoted as LIF266-BP320. Figure 2a shows the signal profiles using this detection scheme along the centreline of the burner (representing small PAHs (2–3 rings) [40, 42, 44, 45]) for various concentration cases of KCl and NaCl salts along with the reference case. Above 5 mm all signal profiles overlap within the experimental uncertainties, hence both salts at all three concentrations negligibly influence the formation of small PAHs at higher HABs in comparison with the reference case. Likewise, Fig. 2b shows the height profiles of 1 M cases of all the salts (KCl, KOH, K_2CO_3, NaCl and NaOH) and the reference case. The similarity between the profiles (above 5 mm HAB) lead us to the conclusion that varying the anion in the salt does not seem to influence the concentration of small PAHs at higher HABs. In our previous study, it was also observed that KCl addition negligibly influence the formation of smaller PAHs (2–3 rings) [28].

In Fig. 2a and b, the PAH-LIF signal intensities show a fast rise to reach a maximum (at around 2–5 mm HAB), to subsequently decrease with increase in HAB. One can observe various delays in the rise in the PAH-LIF signal at lower HABs for the higher concentration cases of the salts (Fig. 2a) as well as for different anions in the salt (Fig. 2b). This behaviour will be discussed in detail in Sect. 3.4.

3.2 Excitation at 532 nm

Figure 3a shows the laser-induced fluorescence signal after excitation using 532 nm (LIF532) along the centreline of the burner (representing larger PAHs [36]) for the various concentration cases of KCl and NaCl along with the reference case. In general, the signal starts appearing at ~ 4–5 mm HAB and increases steadily to attain a maximum at ~ 7–8 mm HAB. The variation of the LIF532 signal for the KCl cases were presented in our previous work [28]. The trends in the peak signal intensities for NaCl cases are similar to those of KCl cases, where the peak PAH-LIF signal decreased with increase in the concentration of added salt. However, with further increase in HAB, the signal intensities of NaCl cases remained near the peak values

contrary to the signals for the KCl cases which dropped. Figure 3b shows the LIF532 height profiles of the 1 M case of all the salts along with the reference case. One interesting observation from Fig. 3b is that at HAB > 8 mm, all the potassium salts overlap with each other irrespective of the anion. Likewise, both the sodium salts are found to be overlapping on top of each other indicating that the anion in the salt negligibly influences the formation of larger PAHs. The authors believe that this is the first study which experimentally shows that the anion in a salt negligibly influences the formation of PAHs. However, salt addition seems to delay the formation of larger PAHs as well to higher HABs, and the delays are different for different salts as will be discussed further in Sect. 3.4.

3.3 PAH-LIF spectra (excitation at 266 nm)

Figure 4 shows the PAH-LIF spectra at 14 mm HAB obtained after the excitation at 266 nm for the 1 M cases of all salts along with the reference case. In the spectra, one can observe a small peak at ~ 350 nm and a larger peak at around 550 nm. As reported in the literature, the peak in the UV region corresponds to small PAHs (2–3 rings) [40, 42, 44, 45]. It can be seen that the low signal in the UV region remains fairly unchanged with the addition of salts, indicating that salt addition does not influence the formation of small PAHs at 14 mm HAB. PAH species such as naphthalene [33, 35, 38, 41], phenanthrene [34, 35] and acenaphthalene [37] are found to have fluorescence peaks in the UV region upon the excitation at 266 nm.

The fluorescence signal in the visible region in Fig. 4 corresponds to larger PAHs or PAH dimers [40, 42, 44–46]. For example, benzoperylene, perylene, fluoranthene and acenaphthalene have peaks in this region [34]. In addition, dimers of pyrene, benzo(a)pyrene and perylene were also found to have peaks in the visible region of the spectra [46].

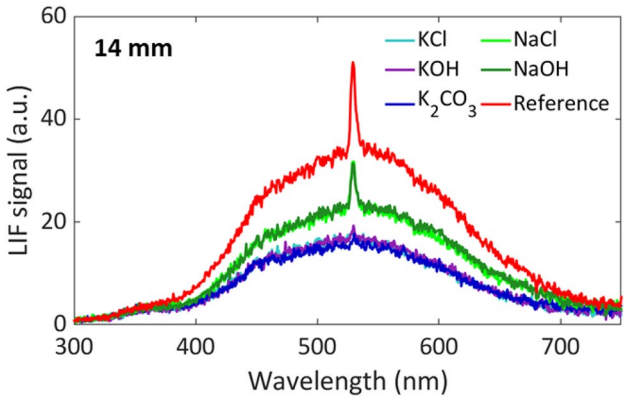

Fig. 4 Laser-induced fluorescence spectra using the excitation wavelength at 266 nm for the 1 M cases of all salts along with the reference case at 14 mm HAB

More details on the types of PAHs based on their fluorescence emission has been given in our previous work [28]. Observing the visible part of the spectra in Fig. 4, one can notice that salt addition reduces the concentration of larger PAHs. One of the most interesting observations from Fig. 4 is that irrespective of the anions, PAH-LIF spectra of all potassium salts overlap well with each other, while the same can be said about sodium salts. This once again suggests that the anion in our tested salts do not have a significant influence in PAH formation at higher HABs. Furthermore, with respect to the reference case, potassium salts show a larger drop in the PAH-LIF signal intensity in the visible range when compared to sodium salts. It can also be seen that the spectral shape in the visible region is fairly unaffected by the addition of salts.

One can observe a sharp peak in the spectra at 532 nm. This is due to the soot particles scattering the small component of unwanted 532 nm radiation superimposed with the 266 nm laser beam. The strength of the signal is much stronger for the reference case compared to the sodium and even absent for the potassium cases. The decrease in scattering signal for Na salt cases is due to the decrease in soot volume fraction as observed by Simonsson et al. [26, 27]. However, for the K salt cases, the compounded effect of decrease in soot volume fraction and decrease in soot particle size results in an almost negligible scattering peak at 532 nm though measurements were performed using the same laser settings. It was also verified that the low intensity 532 nm radiation gave negligible contribution to the total fluorescence shown in Fig. 4.

3.4 Elastic light scattering (ELS)

Elastic light scattering (ELS) from soot is strongly size (d) dependent, such that it is proportional to d^6, and ELS from soot clearly dominates over ELS from molecules at the higher heights (> 10 mm) in the studied flames. Figure 5

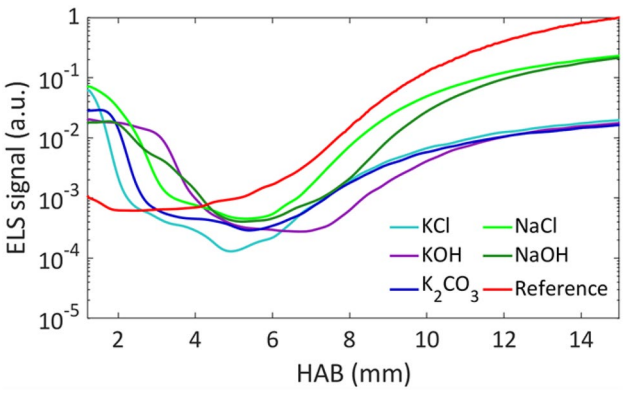

Fig. 5 Variation of elastic light scattering with height above burner for 1 M cases of all salt cases along with the reference case

shows the height profiles of ELS signal intensities for the 1 M cases of all salts along with the reference case in log-lin scale. One of the most interesting results from Fig. 5 is that irrespective of the anion, the ELS signal profiles of all potassium salt cases overlap with each other at higher HABs (HAB $\gtrsim$ 10 mm). The same can be stated about both of the sodium salt cases as well. As the ELS signal at higher HABs is clearly attributed soot particles, it can be implied that the anion in the salt do not significantly influence even the soot formation at higher HABs. With respect to the reference case, potassium salt cases show a larger decrease in ELS signals than the sodium salt cases. This could be primarily due to the decrease in soot particle sizes upon the addition of potassium salts as shown by Simonsson et al. for KCl [26, 27]. However, for the sodium salt cases, the decrease in ELS signals could be primarily due to the decrease in soot volume fraction as there was no significant change in primary particle size [26, 27].

One can also observe high scattering signals at lower HABs (~ 1–3 mm) for the salt added cases in Fig. 5, which give ELS contributions at least one order of magnitude above the reference case. This signal most likely originates from salt particles formed after the vaporization of the solvent (water), as other potential sources can be ruled out based on experimental observations. For example, due to the small transmission range of the band-pass filter used for ELS measurements (3 nm), the fluorescence contribution from the PAHs can be neglected. Scattering contribution from PAH molecules can also be considered to be minimal, as the trends with HAB for the PAHs seen in Figs. 2 and 3 do not match with Fig. 5. In addition, this signal could not have been from soot as soot formation begins at HABs ~ 4 mm.

We do not fully understand the variation in the observed delay of the onset of PAH signals for the studied cases in Figs. 2 and 3. It could possibly be a temperature effect, and it was found in measurements by Simonsson et al. that the temperature difference between the 1 M KCl and the reference cases between the HABs 2–6 mm could be up to 20 K [26, 27]. However, despite these differences in the delays for different anions in the salt, the ELS signal intensities (as well as PAH-LIF intensities in Sects. 3.1–3.3) reach the same values at higher HABs.

3.5 Discussion

From results presented in Figs. 2 and 3, one can state that potassium and sodium salts negligibly affect the formation of smaller PAHs while reducing the concentration of larger PAHs at higher HABs. This indicates that metal salts act in a way to hinder the progression of small PAHs to larger ones. This has been reported in previous studies for the addition of K_2CO_3 [7] and for KCl in our previous study [28]. In an earlier study, Elliot et al. [12] found that when biomass was impregnated with K_2CO_3, a significantly larger decrease in concentration was observed for heavier PAHs (3 rings) when compared to light aromatic tar (1 ring). However, there has been some studies which showed contrasting results compared to the present investigation. Addition of potassium hydroxide (KOH) to lean toluene flames has been shown to considerably increase solid phase PAHs while slightly increasing gas phase PAHs [47]. The enhanced PAH formation is suggested to be due to the partial oxidation of soot in the secondary flame zone. Furthermore, another recent study on coal-derived soot showed that Na in pyrolysis gas promoted the aggregation of aromatic compounds, potentially through Na^+–π interactions to increase the soot yield [15]. In yet another study, it was shown that at low temperatures Na^+ promoted the aggregation of small PAH molecules, while inhibited the same at higher temperatures (> 1373 K) due to the dominance of catalytic effects [17]. This shows that flame conditions like temperature and local equivalence ratios significantly influence the chemistry of PAH and soot formation upon the addition of metal salts.

Another important observation from this study is that the PAH and soot formation at higher HABs seem to be independent of the type of anion in the salt, and seems to depend significantly on the cation in the salt. In the literature, fundamental investigations on the effects of metal additives on soot and especially PAH formation performed using different anions in potassium or sodium salts are scarce. In an earlier study by Mitchell and Miller, it was found that soot burnout rates were independent of the anion (Cl^- and NO_3^{2-}) in the salt [48]. A study on the effects of metal additives on the combustion of polystyrene showed that anions such as Cl^-, CO_3^{2-} and NO_3^{2-} had no detectable differences on the soot yield [49]. The present study can be useful in improving the chemical kinetic models related to the influence of alkali metal additives on soot formation while improving the fundamental understanding on this process.

4 Conclusions

In this study, the influence of addition of potassium salts (KCl, KOH and K_2CO_3) and sodium salts (NaCl and NaOH) to premixed ethylene–air flames ($\Phi = 2.6$) has been investigated primarily using laser-induced fluorescence of polycyclic aromatic hydrocarbons (PAH-LIF). The main conclusions of this study are:

1. Salt addition negligibly influences the formation of small PAHs (2–3 rings). Small PAHs were formed at low HABs (~ 1–2 mm) and showed a steep rise in concentration to reach a maximum at ~ 3–4 mm HAB. The PAH-LIF signal decreased with further increase in HAB.

2. Salt addition reduces the formation of larger PAHs, and increasing concentration of salts successively reduces the concentration of larger PAHs. Larger PAHs were formed at higher HABs (~4–5 mm) and reached a maximum at ~7–8 mm HAB. The reference and sodium salt cases maintained signal intensities close to their respective maxima with further increase in HAB, while the PAH-LIF intensities for the potassium salt cases showed a decrease.
3. The shape of the PAH-LIF spectra were found to be unaffected by salt addition.
4. The anion in the salt (Cl^-, OH^-, CO_3^{2-}) was found to have negligible influence in the PAH and soot formation, since the height profiles at higher flame heights of all the PAH-LIF and scattering signals from the potassium salts overlapped with each other, whereas the same observation was made for both the sodium salts.

Acknowledgements This project was financially supported by the Swedish Energy Agency through the Swedish Gasification Centre (SFC) (34721-3).

Author contributions Conceptualization and methodology: MM, SB and P-EB. Investigation, data curation and validation: MM and SB. Formal analysis, software, visualization, and 'writing—original draft': MM. Funding acquisition, project administration, and supervision: P-EB. Writing—review and editing: SB and P-EB. All authors have read and agreed to the submitted version of the manuscript.

Funding Open access funding provided by Lund University.

References

1. H. Michelsen, Probing soot formation, chemical and physical evolution, and oxidation: a review of in situ diagnostic techniques and needs. Proc. Combust. Inst. **36**(1), 717–735 (2017)
2. H. Wang, Formation of nascent soot and other condensed-phase materials in flames. Proc. Combust. Inst. **33**(1), 41–67 (2011)
3. H. Michelsen, C. Schulz, G. Smallwood, S. Will, Laser-induced incandescence: particulate diagnostics for combustion, atmospheric, and industrial applications. Prog. Energy Combust. Sci. **51**, 2–48 (2015)
4. Q. He, Q. Guo, K. Umeki, L. Ding, F. Wang, G. Yu, Soot formation during biomass gasification: a critical review. Renew. Sustain. Energy Rev. **139**, 110710 (2021)
5. A. Ferreiro, R. Segurado, M. Costa, Modelling soot formation during biomass gasification. Renew. Sustain. Energy Rev. **134**, 110380 (2020)
6. X. Wang, S. Bai, Q. Jin, S. Li, Y. Li, Y. Li, H. Tan, Soot formation during biomass pyrolysis: effects of temperature, water-leaching, and gas-phase residence time. J. Anal. Appl. Pyrol. **134**, 484–494 (2018)
7. A. Bach-Oller, E. Furusjö, K. Umeki, On the role of potassium as a tar and soot inhibitor in biomass gasification. Appl. Energy **254**, 113488 (2019)
8. A. Trubetskaya, F.H. Larsen, A. Shchukarev, K. Ståhl, K. Umeki, Potassium and soot interaction in fast biomass pyrolysis at high temperatures. Fuel **225**, 89–94 (2018)
9. L. Sandström, A.-C. Johansson, H. Wiinikka, O.G. Öhrman, M. Marklund, Pyrolysis of Nordic biomass types in a cyclone pilot plant—Mass balances and yields. Fuel Process. Technol. **152**, 274–284 (2016)
10. A.D. Paulsen, T.A. Kunsa, A.L. Carpenter, T.J. Amundsen, N.R. Schwartz, J. Harrington, J. Reed, B. Alcorn, J. Gattoni, P.E. Yelvington, Gaseous and particulate emissions from a chimneyless biomass cookstove equipped with a potassium catalyst. Appl. Energy **235**, 369–378 (2019)
11. A. Carrascull, I.D. Lick, M.I. Ponzi, E.N. Ponzi, Diesel soot combustion. KNO 3 and KOH catalysts supported on zirconia. React. Kinet. Catal. Lett. **94**(1), 91–98 (2008)
12. D.C. Elliott, E.G. Baker, The effect of catalysis on wood-gasification tar composition. Biomass **9**(3), 195–203 (1986)
13. K. Kirtania, J. Axelsson, L. Matsakas, P. Christakopoulos, K. Umeki, E. Furusjö, Kinetic study of catalytic gasification of wood char impregnated with different alkali salts. Energy **118**, 1055–1065 (2017)
14. P. Ma, Q. Huang, Q. Gao, S. Li, Effects of Na and Fe on the formation of coal-derived soot in a two-stage flat-flame burner. Fuel **265**, 116914 (2020)
15. H. Dong, Q. Du, D. Li, D. Feng, J. Gao, S. Wu, Impact of sodium on the formation mechanism and physicochemical properties of coal-derived soot. Energy Fuels **34**(2), 1453–1466 (2020)
16. Y. Du, W. Lin, P. Glarborg, Particulate emissions from a modern wood stove–Influence of KCl. Renew. Energy **170**, 1215–1227 (2021)
17. H. Dong, Y. Zhang, Q. Du, D. Li, D. Feng, J. Gao, S. Wu, Effect of different forms of Na and temperature on soot formation during lignite pyrolysis. Fuel **280**, 118514 (2020)
18. S. Deng, X. Wang, J. Zhang, Z. Liu, H. Mikulčić, M. Vujanović, H. Tan, N. Duić, A kinetic study on the catalysis of KCl, K2SO4, and K2CO3 during oxy-biomass combustion. J. Environ. Manage. **218**, 50–58 (2018)
19. S. Di Stasio, J.-L. LeGarrec, J. Mitchell, Synchrotron radiation studies of additives in combustion, II: Soot agglomerate microstructure change by alkali and alkaline-earth metal addition to a partially premixed flame. Energy Fuels **25**(3), 916–925 (2011)
20. B. Haynes, H. Jander, H.G. Wagner, editors. The effect of metal additives on the formation of soot in premixed flames, in Symposium (international) on Combustion; 1979: Elsevier.
21. Y. Du, P. Glarborg, W. Lin, Influence of potassium on benzene and soot formation in fuel-rich oxidation of methane in a laminar flow reactor. Combust. Flame **234**, 111624 (2021)
22. M. Kazemimanesh, A. Baldelli, U. Trivanovic, O. Popovicheva, M. Timofeev, N. Shonija, Y. Obvintsev, C. Kuang, A.M. Jefferson, J.C. Corbin, Particulate emissions from turbulent diffusion flames with entrained droplets: a laboratory simulation of gas flaring emissions. J. Aerosol Sci. **157**, 105807 (2021)

23. Z. Xiao, Y. Tang, J. Zhuo, Q. Yao, Effect of the interaction between sodium and soot on fine particle formation in the early stage of coal combustion. Fuel **206**, 546–554 (2017)
24. H. Bladt, N.P. Ivleva, R. Niessner, Internally mixed multicomponent soot: Impact of different salts on soot structure and thermochemical properties. J. Aerosol. Sci. **70**, 26–35 (2014)
25. M. Kazemimanesh, C. Kuang, L.W. Kostiuk, J.S. Olfert, Effect of sodium chloride on the evolution of size, mixing state, and light absorption of soot particles from a smoking laminar diffusion flame. Combust. Flame **218**, 168–178 (2020)
26. J. Simonsson, N.-E. Olofsson, H. Bladh, M. Sanati, P.-E. Bengtsson, Influence of potassium and iron chloride on the early stages of soot formation studied using imaging LII/ELS and TEM techniques. Proc. Combust. Inst. **36**(1), 853–860 (2017)
27. J. Simonsson, N.-E. Olofsson, A. Hosseinnia, P.-E. Bengtsson, Influence of potassium chloride and other metal salts on soot formation studied using imaging LII and ELS, and TEM techniques. Combust. Flame **190**, 188–200 (2018)
28. M. Mannazhi, S. Bergqvist, P.-E. Bengtsson, Influence of potassium chloride on PAH concentration during soot formation studied using laser-induced fluorescence. Combust. Flame **2021**, 111709 (2021)
29. J. Huang, S.M. Senkan, editors. Polycyclic aromatic hydrocarbon and soot formation in premixed flames of CH3Cl/CH4 and CH4, in Symposium (International) on Combustion; 1996: Elsevier.
30. A. Violi, A. D'Anna, A. D'Alessio, A modeling evaluation of the effect of chlorine on the formation of particulate matter in combustion. Chemosphere **42**(5–7), 463–471 (2001)
31. P. Desgroux, X. Mercier, K.A. Thomson, Study of the formation of soot and its precursors in flames using optical diagnostics. Proc. Combust. Inst. **34**(1), 1713–1738 (2013)
32. S. Bejaoui, X. Mercier, P. Desgroux, E. Therssen, Laser induced fluorescence spectroscopy of aromatic species produced in atmospheric sooting flames using UV and visible excitation wavelengths. Combust. Flame **161**(10), 2479–2491 (2014)
33. Y. Zhang, Y. Li, L. Wang, P. Liu, R. Zhan, Z. Huang, H. Lin, Investigation on the LIF spectrum superposition of gas-phase PAH mixtures at elevated temperatures: potential for the analysis of PAH LIF spectra in sooting flames. Appl. Phys. B **125**(5), 72 (2019)
34. F. Beretta, V. Cincotti, A. D'alessio, P. Menna, Ultraviolet and visible fluorescence in the fuel pyrolysis regions of gaseous diffusion flames. Combust. Flame **61**(3), 211–218 (1985)
35. F. Ossler, T. Metz, M. Aldén, Picosecond laser-induced fluorescence from gas-phase polycyclic aromatic hydrocarbons at elevated temperatures. I. Cell measurements. Appl. Phys. B **72**(4), 465–478 (2001)
36. I. Berlman, Handbook of fluorescence spectra of aromatic. Molecules **1971**, 5 (1971)
37. L. Petarca, F. Marconi, Fluorescence spectra and polycyclic aromatic species in a n-heptane diffusion flame. Combust. Flame **78**(3–4), 308–325 (1989)
38. G. Zizak, F. Cignoli, G. Montas, S. Benecchi, R. Donde, Detection of aromatic hydrocarbons in the exhaust gases of a gasoline ic engine by laser-induced fluorescence technique. Rec. Res. Dev. Appl. Spectrosc **1**, 17–24 (1996)
39. A. D'Alessio, A. D'Anna, A. D'orsi, P. Minutolo, R. Barbella, A. Ciajolo, editors. Precursor formation and soot inception in premixed ethylene flames, in Symposium (International) on Combustion; 1992: Elsevier
40. A. Ciajolo, R. Ragucci, B. Apicella, R. Barbella, M. De Joannon, A. Tregrossi, Fluorescence spectroscopy of aromatic species produced in rich premixed ethylene flames. Chemosphere **42**(5–7), 835–841 (2001)
41. A. Ciajolo, A. Tregrossi, R. Barbella, R. Ragucci, B. Apicella, M. De Joannon, The relation between ultraviolet-excited fluorescence spectroscopy and aromatic species formed in rich laminar ethylene flames. Combust. Flame **125**(4), 1225–1229 (2001)
42. P. Liu, Z. He, G.-L. Hou, B. Guan, H. Lin, Z. Huang, The diagnostics of laser-induced fluorescence (LIF) spectra of PAHs in flame with TD-DFT: special focus on five-membered ring. J. Phys. Chem. A **119**(52), 13009–13017 (2015)
43. L. Sgro, P. Minutolo, G. Basile, A. D'Alessio, UV-visible spectroscopy of organic carbon particulate sampled from ethylene/air flames. Chemosphere **42**(5–7), 671–680 (2001)
44. A. Ciajolo, R. Barbella, A. Tregrossi, L. Bonfanti, editors. Spectroscopic and compositional signatures of PAH-loaded mixtures in the soot inception region of a premixed ethylene flame, in Symposium (International) on Combustion; 1998: Elsevier
45. S. Lee, S. Yoon, S. Chung, Synergistic effect on soot formation in counterflow diffusion flames of ethylene–propane mixtures with benzene addition. Combust. Flame **136**(4), 493–500 (2004)
46. X. Mercier, O. Carrivain, C. Irimiea, A. Faccinetto, E. Therssen, Dimers of polycyclic aromatic hydrocarbons: the missing pieces in the soot formation process. Phys. Chem. Chem. Phys. **21**(16), 8282–8294 (2019)
47. Y.-L. Wei, Effect of potassium hydroxide on PAH formation during toluene incineration. Chemosphere **37**(3), 509–521 (1998)
48. J. Mitchell, D. Miller, Studies of the effects of metallic and gaseous additives in the control of soot formation in diffusion flames. Combust. Flame **75**(1), 45–55 (1989)
49. S.-L. Chung, S.-M. Tsang, Soot control during the combustion of polystyrene. J. Air Waste Manag. Assoc. **41**(6), 821–826 (1991)